Electronic Supplementary Material (ESI) for Soft Matter

Supplementary Information

Materials and Methods

Protein purification (FPLC)

The stock solution, typically with ~ 20 mg/ml of polyclonal sheep Immunoglobin G (abbreviated as IgG, Rockland Immunochemicals) was further purified. The solution was passed through a fast protein liquid chromatography column (GE Healthcare HiLoad 16/60 Superdex 200 pg) using a buffer at pH 7 (100 mM phosphate and 300 mM NaCl) as the mobile phase. The monomer fractions observed with absorbance at 280 nm were collected and pooled, and the oligomers were discarded.

Buffer exchange

After the FPLC purification step, the ~4 mg/ml solution of polyclonal sheep IgG was buffer exchanged into 50 mM phosphate buffer with the desired amount of dissolved trehalose (typically 70-125 mg/ml). The buffer was formulated at the isoelectric point (pI) of the protein, which is 6.4 for the polyclonal sheep IgG. The buffer exchange was carried out using centrifugal filter tubes (Millipore, Amicon Ultracell 30K centrifugal filters) with a molecular weight cutoff of 30 kDa and a capacity of 12 ml. A desired amount (typically 6-8 ml) of the protein solution was added to the filter tube and the volume was increased to 12 ml using the desired buffer for the dispersion. The buffer was forced through the membrane by centrifugal filtration at 4500 radial centrifugal force (rcf) for 12 minutes concentrating the protein solution in the retentate until the solution volume dropped to about 2 ml. Then the retentate protein solution was again diluted to 12 ml in the same buffer as before and concentrated down to 2 ml again. The dilution and centrifugation process was repeated 4 or more times until the permeate volume was 4-5 times the original solution volume, typically 40 ml. After buffer exchange, the solution was further concentrated so that the final solution volume was about 0.5 ml.

Centrifugal filtration of protein solution to form a dispersion of nanoclusters upon concentration

Tare weights were taken of a centrifugal filter assembly (Millipore Microcon, Ultracel YM-50 membrane, 50 kDa nominal molecular weight limit, diameter of filter, 0.25”). The desired

volume (~0.5 ml) of protein solution, after buffer exchange and concentration, was pipetted into the retentate chamber. The filter assembly was then centrifuged (Eppendorf Centrifuge 5415D) at 10,000 rcf typically in about 20-40 minute increments until the calculated final retentate volume for the desired final protein concentration was reached. The volume measurements were done using image analysis (ImageJ software) to determine the height of the liquid column in the retentate chamber. Additionally, the protein concentration in the retentate dispersion was determined by measuring out 2 µl (± 0.08 µl) of dispersion using an Eppendorf Research adjustable volume 0.5-10 µl pipette and diluting it into a receiving vessel containing 998 µl of the same buffer. For mixing, the solution was cycled 5 times into and back out of the pipette tip followed by light agitation with the pipette tip. The absorbance of the resulting solution at 280 nm was measured using a Cary 3E uv-visible spectrophotometer in a cuvette (Hellma cells) with a path length of 1 cm, and converted to concentration assuming an extinction coefficient of 1.43 ml mg^{-1} cm^{-1}.

Once the desired concentration had been reached, the dispersion of protein nanoclusters in the retentate chamber was recovered by inverting the filter assembly into a retentate recovery tube, and centrifuging it for 3-4 minutes at 1,000 rcf. The resulting dispersion was transferred to a 0.1 mL conical vial (V-Vial, Wheaton), and the concentration was confirmed using 2µl of the dispersion as described above.

Characterization of the protein nanocluster dispersion

Hydrodynamic diameters

The short-time mutual diffusion coefficient $D_s(q)$ of protein nanoclusters was extracted from intensity correlation functions measured using dynamic light scattering. Measurements were taken at angle of 150° with a 632.8 nm laser (q = 0.01918 nm^{-1}) and an avalanche photodiode at ~23°C using a custom apparatus (Brookhaven BI-9000AT and 60 µl Beckman Coulter sample cell)[1] and analyzed with the CONTIN algorithm (volume distribution). Hydrodynamic cluster diameters D_c were estimated from the $D_s(q)$ using Beenakker-Mazur theory[2] for $D_s(q)/D_0$, where $D_0 = kT / 3\pi\eta D_c$ and η is the shear viscosity of the buffer solvent with added excipients. This approach assumes that the protein clusters act like suspended hard spheres occupying an effective packing fraction $\phi_c^{\text{eff}} = \phi/\phi_c^{\text{int}}$, where ϕ_c^{int} is the protein packing

fraction within a cluster. In this work, we assumed $\phi_c^{\text{int}} = 0.60$, which is consistent with light scattering data on protein nanoclusters reported previously.[1] We also verified that an alternative approximation, $\phi_c^{\text{int}} = (D_c/2R)^{\delta_f - 3}$ (where δ_f is the fractal dimension, taken as 2.6),[1] resulted in similar cluster size estimates. The measured intensity correlation functions decayed on time scales between ~10 to 50 μs, consistent with short-time diffusion for clusters with the diameters and mobilities reported here.

Size exclusion chromatography

For analysis of non-covalent aggregates, the sample was diluted in mobile phase (100 mM sodium phosphate, 300 mM sodium chloride, pH 7) to ~1 mg/ml. 20 μg of diluted dispersion was analyzed with a Waters Breeze HPLC, using TOSOH Biosciences TSKgel3000SW$_{XL}$ and TSKgel2000SW columns in series, with eluate monitored by absorbance at 214 nm.

Enzyme linked immunosorbent assay (ELISA)

An enzyme-linked immunosorbent assay (ELISA) was performed by coating a 96-well Costar high binding polystyrene plate with anti-polyclonal sheep IgG (Sigma) in PBS at 1 μg/ml at 4°C overnight. The sheep IgG samples were serially diluted in a 1:5 ratio starting at 10 μg/ml. The plate was then blocked with 5% milk in PBS for two hours at room temperature. Bound IgG was detected with anti-polyclonal sheep IgG conjugated with horseradish peroxidase (Sigma) in PBS added to each well in a 1:5000 ratio. The signal was developed with a TMB solution (Thermo Scientific) and the reaction was quenched with 1N HCl. The signal was detected using a spectrophotometer (Molecular Devices Spectramax M5) at an absorbance of 450 nm. The data was fit to a four parameter logistic curve (MATLAB nonlinear curve fitting) and the half maximal effective concentration (EC50) reported.

Circular dicroism (CD)

Secondary structure was determined by diluting the dispersions to approximately 10 mg/ml in 5 mM phosphate buffer at pH 7.4. The samples were then placed in the JASCO J-815 circular dichroism (CD) spectrometer and the CD spectrum was measured from 260 nm to 190

nm. Data was analyzed with Dichroweb online analysis tool, using the CDSSTR function and reference set 4.[3]

Viscosity

The viscosities of the nanocluster dispersions were measured in triplicate using a 25 gauge (ID = 0.1 mm) 1.5" long needle (Becton Dickinson & Co. Precision Glide Needle) attached to a 1 ml syringe (Becton Dickinson & Co. 1 mL syringe with Luer-Lok™ tip), according to the Hagen-Poiseuille equation.[1] The flow rate of the dispersion through the needle was determined by correlating volume to the height of the liquid in the conical vial (using ImageJ software) and measuring the time taken for the dispersion column height to move between two points. The flow rate was correlated to viscosity from a calibration curve derived from a set of standards of known viscosities.[1]

Equilibrium model for cluster formation

The model we use here is based on an approach originally introduced to qualitatively understand cluster formation of colloids suspended in apolar solvents.[10, 11] Specifically, we adopt a generalization put forth by Johnston et al.[1] to study aqueous, protein nanocluster dispersions which accounts for the fractal dimension of the clusters and the possibility of tunable depletion interactions.

The model assumes a hierarchy of multi-scale interactions that drive the formation of clusters shown schematically in Fig. 1a. Here, the primary attraction between protein monomers is assumed to be an osmotic depletion force induced by the presence of an extrinsic crowding co-solute (in this case, trehalose). The origin of the depletion attraction is entropic. Configurations where two protein molecules are in contact are favored statistically over those in which the proteins are separated in solution because the former excludes trehalose molecules from a smaller overall volume. Since the diameter of a trehalose molecule is considerably smaller than that of a protein monomer, the interprotein depletion interaction is short-ranged. This kind of depletion attraction is commonly described by the Asakura-Oosawa effective pair potential[4,5]

$$\frac{V_{dep}}{k_B T} = -\frac{\phi_E}{2}\left(1 - \frac{r - 2R}{2R_E}\right)^2 \left(2 + \frac{3R}{R_E} + \frac{r - 2R}{2R_E}\right) \quad \text{(S1)}$$

where r is the center to center distance between two protein molecules, R is the protein molecular radius, ϕ_E is the volume fraction of the extrinsic crowder, and R_E is the crowder radius.[6] Since the strength of the depletion attraction depends on ϕ_E (as is expected for an osmotic attraction), it can be tuned experimentally by modifying the crowder concentration. Depletion attraction due to poly(ethylene glycol) (PEG) has been demonstrated as being the dominant interaction modulating protein-protein interactions for proteins with weakened electrostatic interactions.[7-11] As a result, other short-range attractive interactions arising from hydrogen-bonding, hydrophobic forces, etc., as well as longer-range van der Waals interactions—while also present in the protein system—are assumed to play a secondary role in cluster formation at high crowder concentrations.[1]

Proteins also interact through electrostatic repulsions. In this work, the pH of the solution is adjusted to be near the pI of the protein which minimizes the net charge on the protein molecules.[12] As a result, electrostatic repulsions between two isolated protein monomers in solution are expected to be weak compared to the short-range attractions, especially under conditions of high crowder concentration (see Fig S7). However, as proteins begin to form a cluster (i.e., each protein acquires multiple contacting neighbors), contributions from the weak—but longer-range—electrostatic repulsions begin to accumulate. Qualitatively, the balance between attractions and repulsions determines the equilibrium cluster size. For a discussion of why electrostatic screening inside of the protein clusters may be considerably weaker than that between two proteins isolated in aqueous buffer, see Harada et al[13] and Johnston et al.[1] The aforementioned balance between short-range attractions and longer-range repulsions is expected to produce interactions between equilibrium-size clusters that are net repulsive, which helps create colloidally-stable nanocluster dispersions that do not readily gel.

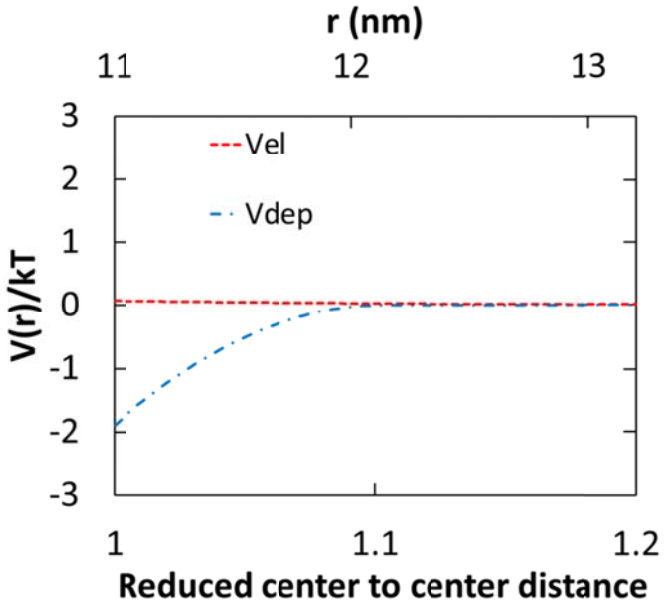

Figure S1. Potential of mean force between two protein monomers at the pI with trehalose concentration 70 mg/ml. V_{dep} is the force due to the depletion attraction from trehalose and V_{el} is the electrostatic repulsion.[1]

In the free energy model for cluster formation, proteins are assumed to assemble into spherical clusters of radius R_c comprising n_c monomers, as shown in Fig. 1a. If the strength of the depletion interaction between two neighboring proteins is given by $-\varepsilon$ and each protein has C nearest neighbors in the cluster interior, then the effective depletion contribution to the free energy per protein molecule in the cluster interior will be $-\varepsilon C/2$. The missing attractive interactions for proteins on the cluster surface are accounted for by adding an effective surface energy term ($4\pi R_c^2\gamma$), where the surface tension is approximated as $\gamma = \varepsilon/4\pi R^2$. Together, the depletion attractions contribute the following to the free energy of cluster formation,

$$F_{att} = -\frac{\varepsilon C n_c}{2} + 4\pi R_c^2 \gamma \qquad \text{(S2)}$$

Assuming that the charges are negligibly screened within the cluster (as discussed earlier[1]), their Coulombic self-energy can be approximated as

$$F_{rep} = \frac{3\lambda k_B T n_c^2 q^2}{5R_c} \qquad \text{(S3)}$$

where λ is the Bjerrum length ($\lambda = e^2/4\pi\epsilon_r\epsilon_0 k_B T$), ϵ_r is the relative permittivity of the medium, ϵ_0 is the vacuum permittivity, and q is the charge per protein monomer.

The cluster free energy also depends upon the translational and combinatorial entropy of the counterion dissociation from the proteins in the cluster to the solution. The final free energy per protein of a cluster is given by[14,15]

$$\frac{f_c}{k_B T} = -\frac{\varepsilon C}{2k_B T} + \frac{4\pi R_c^2 \gamma}{k_B T n_c} + \frac{3\lambda n_c q^2}{5R_c} + 2q\left[ln\left(\frac{q}{q_0}\right) - 1\right] \quad \text{(S4)}$$

where q_o is the charge that minimizes f_c for weakly charged particles in the limit of low zeta potential.[14]

Minimizing with respect to R_c (or n_c) gives the following expression for the equilibrium aggregation number n^*

$$n^* = \frac{10\pi\gamma R^3}{3k_B T\lambda q^2} \quad \text{(S5)}$$

As qualitatively discussed above, clusters are predicted to grow with increasing attractions (□) and shrink with increasing charge q (electrostatic repulsion).

To take into account the porosity of the protein cluster, we modify the original model by expressing the cluster radius as

$$R_c = \left(\frac{n_c}{k}\right)^{\frac{1}{\delta_f}} \quad \text{(S6)}$$

where δ_f is the fractal dimension (estimated from static light scattering experiments of one protein cluster dispersion to be 2.6 from Johnston et al.[1]) and k is a constant of order 1. For $q = q_0$,[1,14] the resulting equilibrium aggregation number is given by

$$n^* = k^{\frac{3}{3-2\delta_f}}\left\{\frac{5(\delta_f - 2)\varepsilon R}{3(\delta_f - 1)k_B T\lambda q_0^2}\right\}^{\frac{\delta_f}{2\delta_f - 3}} \quad \text{(S7)}$$

To connect with experimental observables, we can substitute $\varepsilon = -V_{dep}(2R)$ from the depletion potential of eq. S1 into eq. S7. Furthermore, we can use a prediction, $q_0^2 = (1400 * n_d/cb^3)e^{-2-\lambda/b}$, obtained from a simple statistical mechanical site-binding model[14,15] for the

translational and combinatorial entropy of counterion dissociation accounting for the experimentally determined partial molar density of the protein in the solution of 1400 mg/ml. Here, n_d is the number of dissociable sites on a protein surface, and b is the minimum distance between a counterion and a charge on the protein surface. Combining these relations and eq. S1, S6, and S7 with $\phi_E = c_E/1580$ (1580 is the partial molar density of the trehalose in the solution[16]) yields the following relation for cluster diameter,

$$D_c = 2R\left\{\frac{20\pi(\delta_f-2)R^4b^3e^{2+\lambda/b}c_Ec}{1400*1580*9k^2n_d(\delta_f-1)\lambda}\left[1+\frac{3R}{2R_E}\right]\right\}^{\frac{1}{2\delta_f-3}} \quad \text{(S8)}$$

This relation is presented, in simplified form, as eq. (2) of the main text. Importantly, Equation S8 (parameter values provided in Table S6) captures the experimentally observed trends in cluster diameter with changes in extrinsic crowder concentration and protein concentration (Figs 2a-e). This agreement provides further evidence that the dispersed protein clusters are in an equilibrium state.

Table S1: Model parameters for Sheep IgG. Input variables used in the model proposed by Johnston et al.[1] and used to generate the plots in Figs 1b, 2b, and 2e are provided.

Model parameter	**Value**
Fractal Dimension (δ_f)	2.5
Dielectric constant (ϵ_r)	15
No. of dissociable sites per unit area of colloid surface (σ_s, nm^{-2})	0.2
Distance between opposite charges in an ionic bond (b, nm)	0.22
Radius of the protein monomer (R, nm)	5.5

Turbidity and additional electron microscopy of the dispersion

The turbidity of the dispersion is quantified in Fig. S1 in the visible range (400-700 nm). Low turbidity is seen in the visible region as quantified by an average turbidity of 0.335 cm^{-1} and absorbance of 0.15 for a path length of 1 cm from 400-700 nm. The dispersion appears

transparent to the naked eye, which is highly desirable as a guide during subcutaneous administration of the formulation. The high level of transparency is due to the refractive index of the porous cluster being close to that of the solvent with dissolved trehalose.[1] Also, the small size of the clusters < 100 nm leads to relatively low scattering cross sections. The dispersion has a significant absorbance in the UV region due to the aromatic amino acid residues present in the protein molecules and greater Mie scattering.

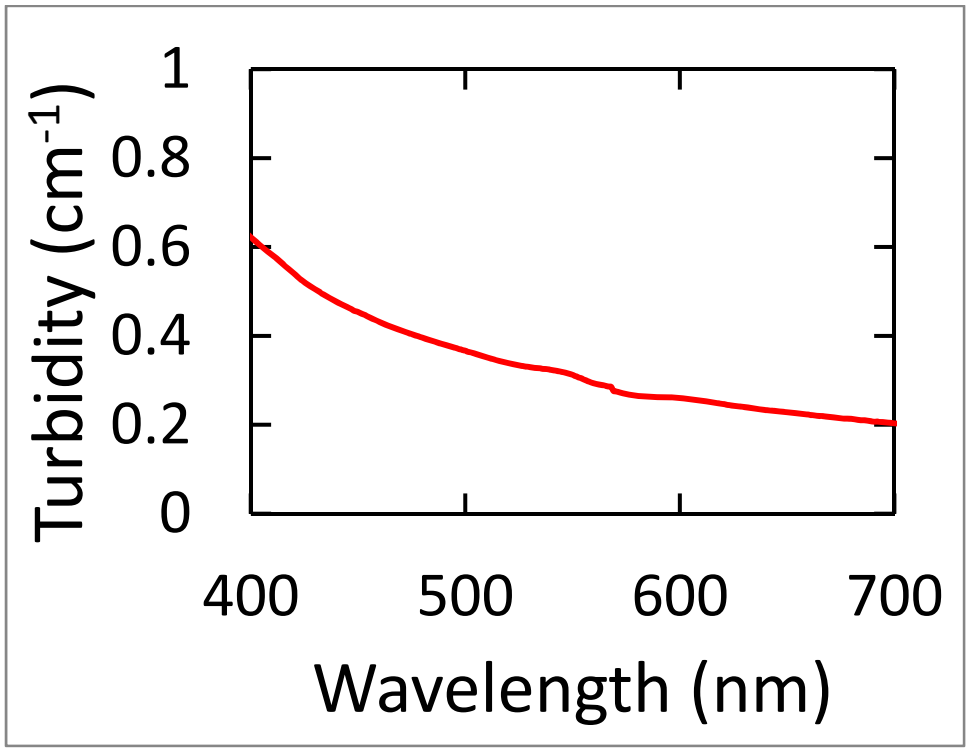

Figure S2: Turbidity of nanocluster dispersion (C 220:70) which appears transparent to the naked eye for a path length of 1 cm.

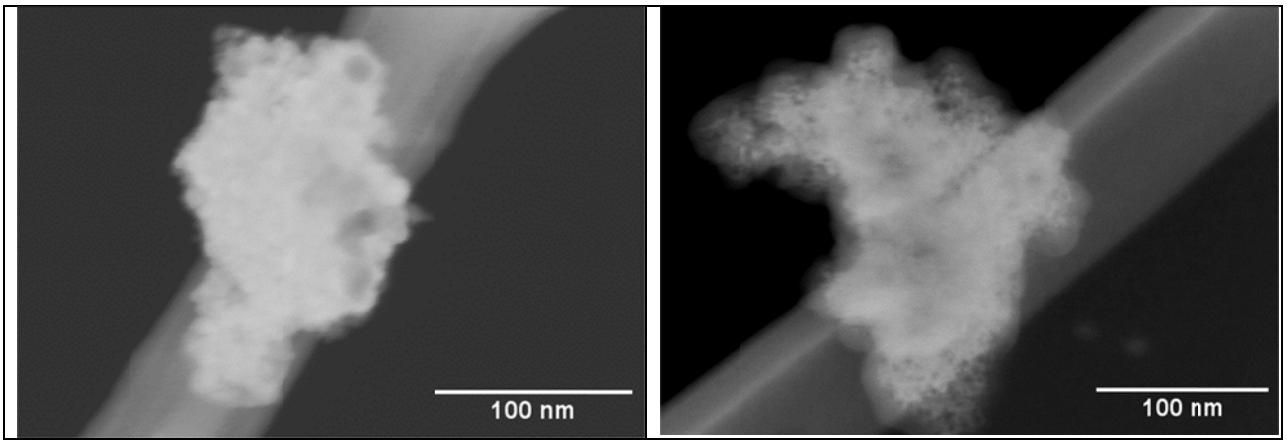

a b

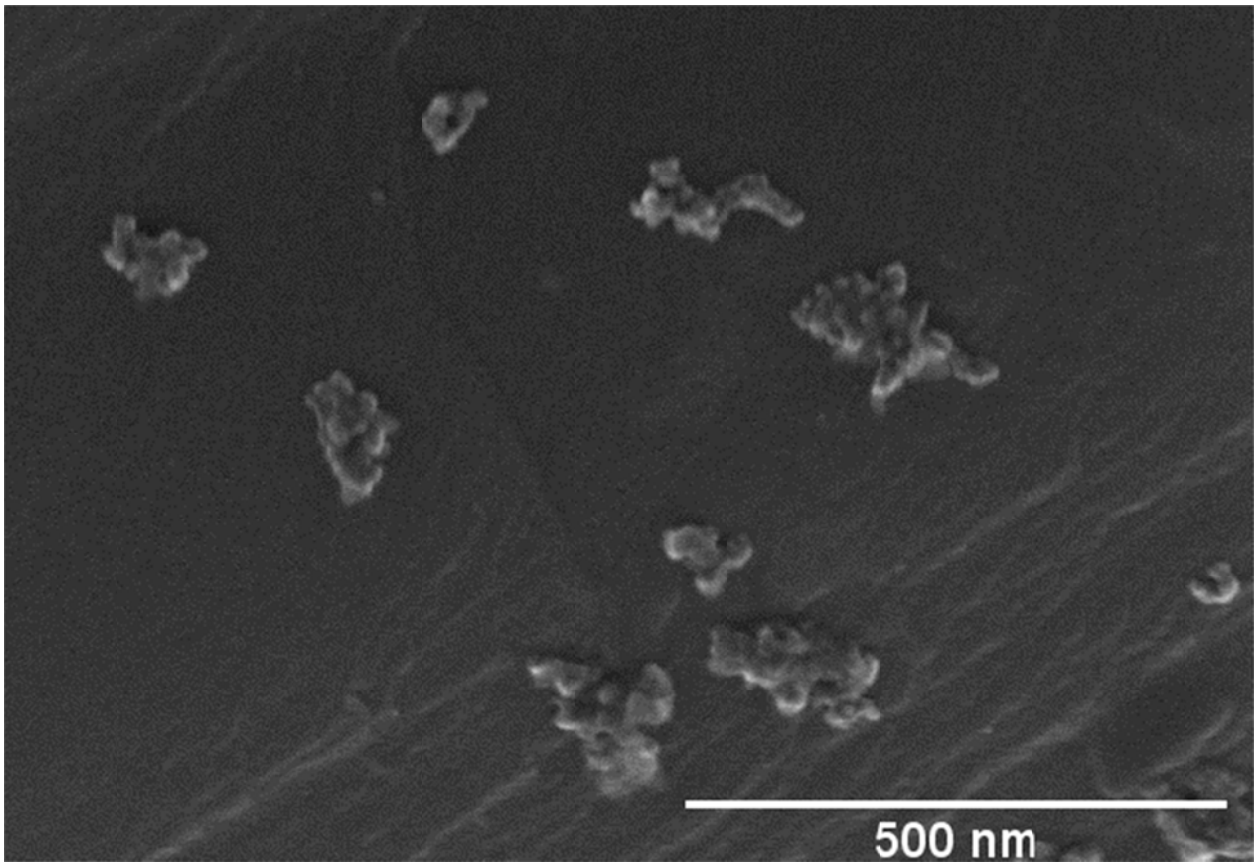

c

Figure S3. Additional STEM (a and b) and SEM (c) images of protein nanoclusters at *c* = 270 mg/ ml and c_E = 270 mg/ml.

Additional dynamic light scattering analysis of the nanoclusters

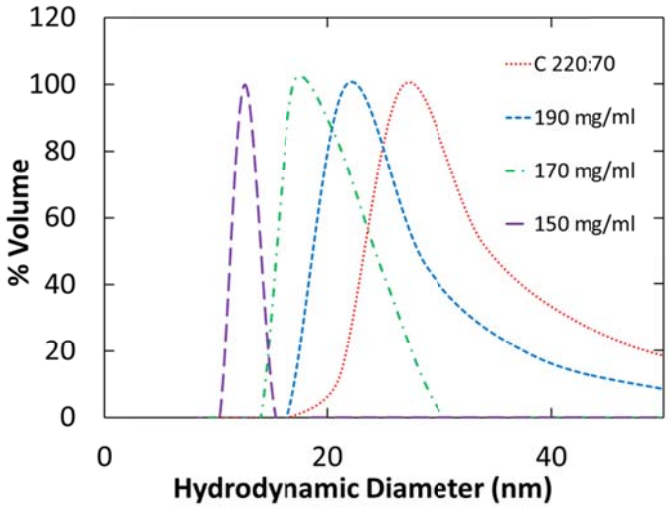

Figure S4: **D_c of C 220:70 nanoclusters and after subsequent sequential dilutions with buffer**. The legend gives the protein concentration with mean D_cs listed in Table S1 and Figs 2b and 2e.

Table S2: **D_c of C 220:70 nanoclusters and after subsequent sequential dilutions with buffer**. The distributions for the D_c are provided in Fig. S3 and the means are in Figs 2b and 2e. The starting solution was at a protein concentration of 70 mg/ml and was centrifuged for 35 minutes.

***c* (mg/ml)**	**D_c (nm)**	**St Dev in D_c (nm)**
220	40	12
190	32	7
170	23	3
150	15	3

Table S3: **D_c of LD 250:100 nanoclusters and after subsequent sequential dilutions with buffer.** The distributions for the D_c are provided in Fig. 2d.

***c* (mg/ml)**	**D_c (nm)**	**St Dev in D_c (nm)**
250	51	9

230	42	7
210	32	5
120	17	9
60	13	4

Dispersions with concentrations of 320 mg/ml

In order to demonstrate the robustness of the clustering concept in general and the centrifugal filtration concept in particular, high concentration dispersions of proteins at a concentration of 320 mg/ml were made with the properties given in Table 1 and Fig. S4. The dispersions had 70 mg/ml trehalose for providing depletion attraction and stability while still maintaining the isotonicity of the dispersion. The dispersions were syringeable as opposed to solutions which typically gel and aggregate at these concentrations.[1] The diameter was observed to be 40 nm relative to a value of 37 for the C 220:70 case in Table 1. In contrast, the model predicts a larger size increase with protein concentration. The protein was found to be monomeric after dilution by SEC despite the high protein concentrations in the dispersions.

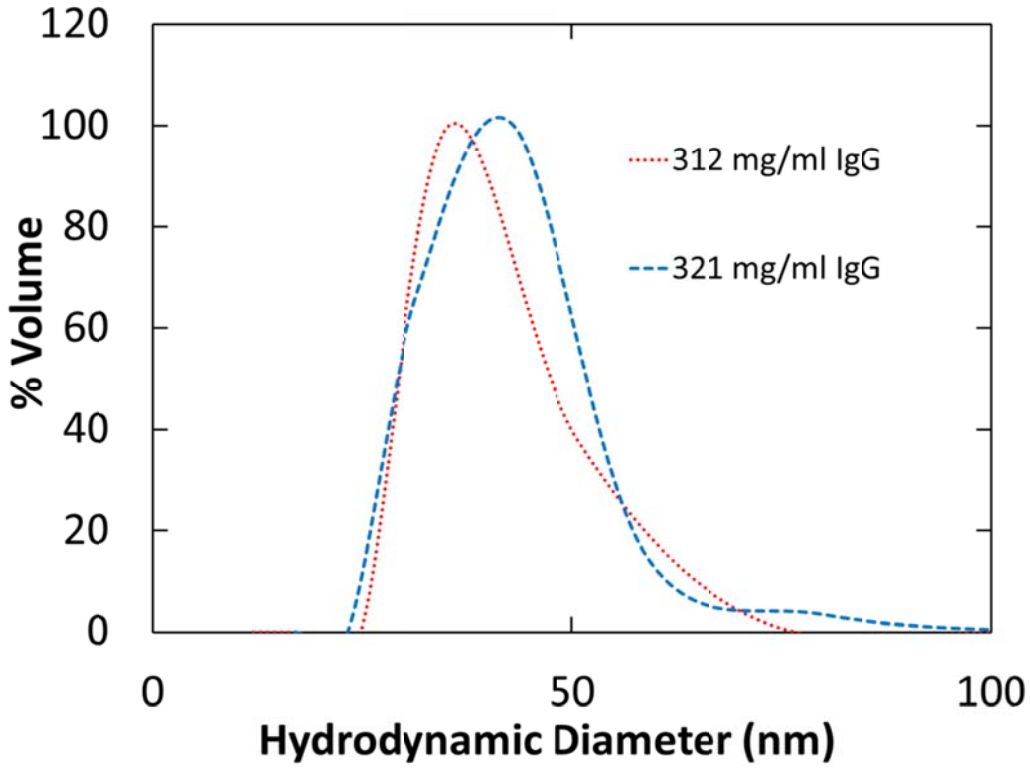

Figure S5. D_c of C 320:70 nanoclusters at an ultra-high protein concentration. The D_c distributions for two different samples are provided with the mean D_c listed in Table 1.

Table S4: **D_c of C 250:250 nanoclusters and after subsequent sequential dilutions with buffer**. The distributions for the D_c are provided in Fig. S5 and the means are in Fig. 2e. The starting solution was at a protein concentration of 50 mg/ml and was centrifuged for 68 minutes.

c **(mg/ml)**	D_c **(nm)**	**St Dev in** D_c **(nm)**
250	77	8
200	59	8
160	43	9
120	18	1
70	11	2
40	12	2.5

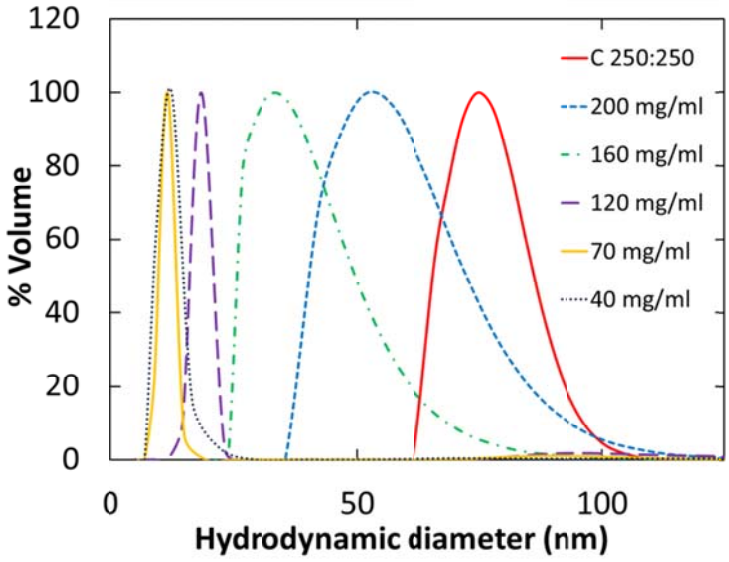

Figure S6. D_c of C 250:250 nanoclusters and after subsequent sequential dilutions with buffer. The legend gives the protein concentration with mean D_cs listed in Table S3 and Fig. 2e.

Room temperature storage stability

Additionally, the dispersions were observed to be stable for 10 days when stored at room temperature with excellent retention of the size and the % monomeric protein upon dilution as

can be seen in Table S4 and Fig. S6. The dispersion also remained clear and there was no phase separation observed during storage, again supporting the concept of nanoclusters at equilibrium.

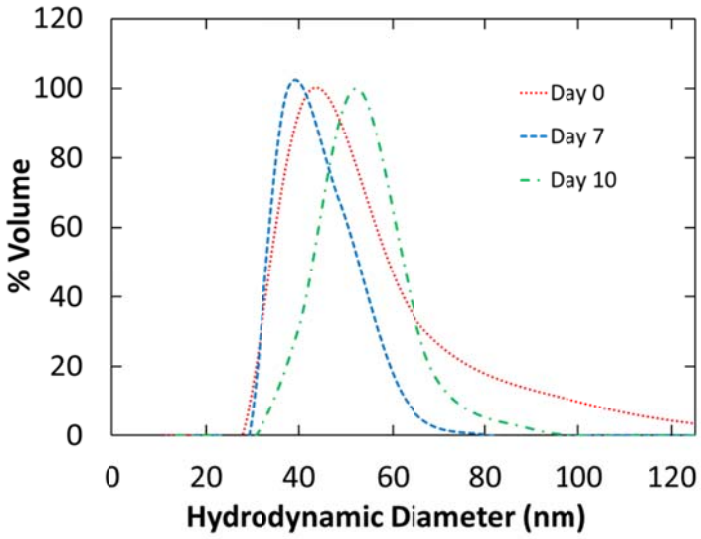

Figure S7. D_c of C 250:100 nanoclusters upon storage of the aqueous dispersion at 23° C for up to 10 days. The mean D_cs are listed in Table S4.

Table S5: D_c, viscosity and protein % monomer after room temperature storage (C 250:100). The distributions for the D_cs are provided in Fig. S6.

Time (days)	**D_c (nm)**	**% monomer by SEC**
0	49 ± 13	98.6
7	44 ± 5	*
10	47 ± 11	98.5

Effect of pH on cluster size

Dispersions were formed at two different pH values of 6.4 (LD 250:100) at the isoelectric point and 6.9 (LD 200:80) to examine the effect of pH on the cluster size. The dispersion properties are contrasted in Table S5. The sizes are seen to be similar at the same protein concentration with the pH having little effect on the dispersion size in this narrow range. The protein charge does not change appreciably within 1 or 2 pH units of the pI leading to the size not changing appreciably as can be seen from equation S7.[12,17] Also, the sheep IgG being

polyclonal has a broader distribution of pIs and hence charge on the protein molecules therefore the charge distribution within the clusters may remain oblivious to pH over a significant range of pH values (2-3 pH units around the pI). These cluster formed at pH 6.9 also dissociated back to monomer upon dilution in buffer.

Table S6: Effect of pH on D_c. LD 200:80 in pH 6.9 and a dilution of LD 250:100 at pH 6.4 are contrasted to observe the effect of protein charge.

Sample name	c_E **(mg/ml)**	c **(mg/ml)**	**dispersion pH**	D_c **(nm)**	**Std. Dev in D_c (nm)**
Dilution of LD 250:100	84	210	6.4	32	5
LD 200:80	80	200	6.9	33	10

ELISA

After analysis of the ELISA data with a four-parameter logistic fit, the relative EC50s were found to be 1.38 ± 0.47 for the LD250:100 sample and 1.13 ± 0.84 for the C 220:70 sample, compared with 1.00 ± 0.36 for the unprocessed sample. After verifying the shape of the sigmoidal curve on the Fig. S8, these were determined to be comparable within one standard deviation. Since this is a capture ELISA using polyclonal antibody mixtures to both capture and detect the sheep IgG molecules, binding depends upon maintenance of multiple epitopes in the sheep antibody structure. If one epitope on each antibody has altered structure, binding would be reduced; alternatively, if a fraction of all antibodies have multiple compromised epitopes, this would also result in decreased binding and higher EC50 values. We thus conclude that the majority of the antigen binding sites are maintained during the centrifugation and lyophilization steps, keeping the protein stable and intact.

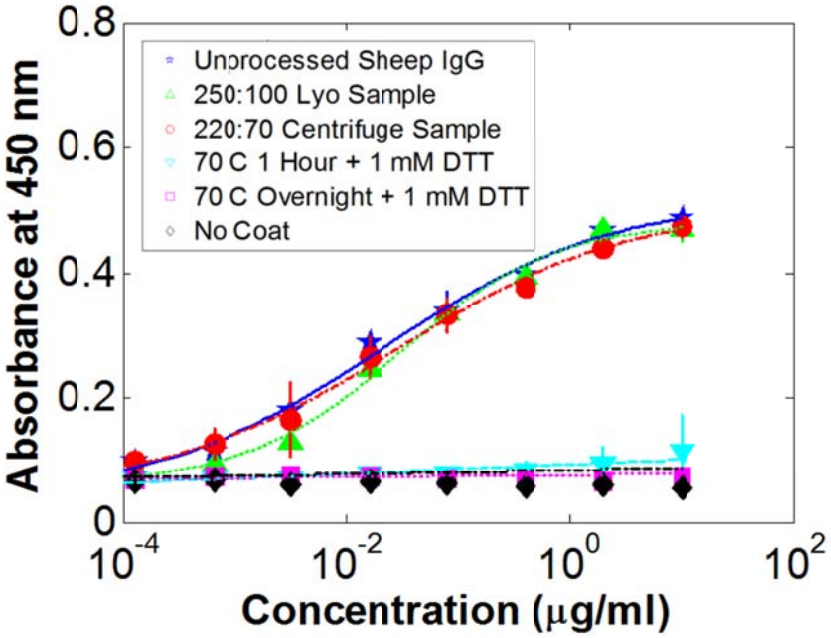

Figure S8. ELISA data for diluted protein samples. The raw data used for calculating the relative EC50 is shown along with the negative controls.

CD

Analysis of the circular dichroism spectra demonstrates maintenance of protein secondary structure throughout the centrifugation, lyophilization and dilution processes. Antibodies are composed primarily of beta sheet secondary structure elements and turns, and the data shows only 3% to 5% alpha helices of the total structure. Circular dichroism provides only an approximation for evaluating secondary structure, but the agreement of the data in Table S7 supports our conclusion based on the ELISA data that antibody structure is maintained throughout the processing steps.

Table S7: Circular Dichroism for protein secondary structure. The fraction of protein in the different secondary structures for both LD and C samples compared to the native protein

Sample	Helix	Strand	Turn	Unordered
Control	0.04	0.18	0.23	0.33
LD 250:100	0.03	0.17	0.22	0.38
C 220:70	0.02	0.19	0.23	0.34

Long term storage

A C 220:70 dispersion was stored at -40ºC for a month and a second dispersion at the same conditions was stored for 2 ½ months. After storage, the dispersions were gently thawed at 4°C and then characterized. The size and viscosity appeared unchanged pre- and post-freezing as is shown in Table S2 and Fig. S4. The constant size provides further evidence the nanoclusters are in an equilibrium state with the size governed by the dispersion composition. The protein is also found to be monomeric by SEC upon dilution with little change in % monomer pre- and post-freezing. The stability after 2 ½ months of storage seems to suggest the potential for long term storage in the frozen state which is a great practical advantage. The stability may result from decreased molecular mobility at low temperatures and the trehalose present in the dispersion acting as a cryoprotectant.[18,19]

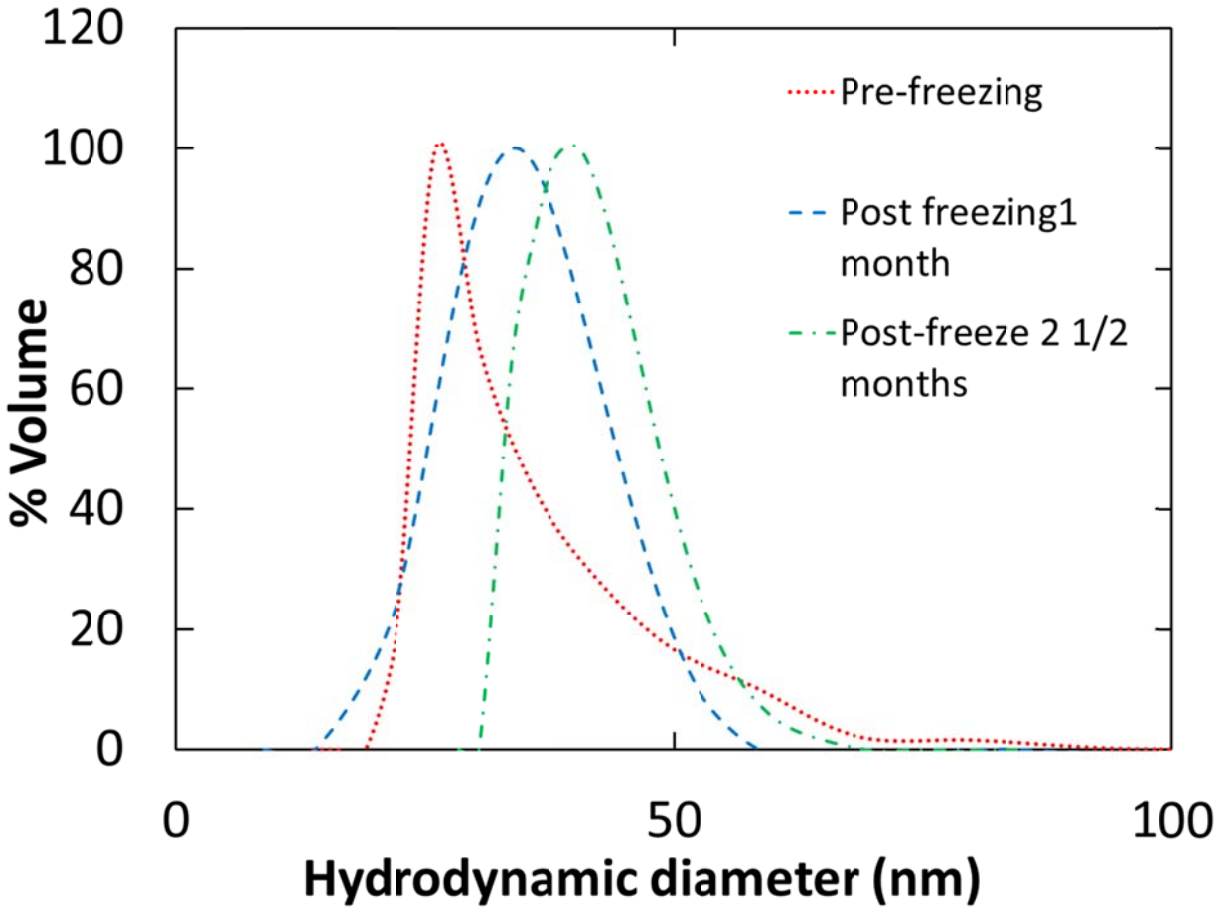

Figure S9: D_cs of C 220:70 nanoclusters before freezing, and after either 1 or 2.5 months of frozen storage at -40^{0}C followed by thawing. The mean D_cs are listed in Table S8.

Table S8: D_c, viscosity and protein % monomer before and after freezing and thawing (C 220:70). The distributions for the D_cs are provided in Fig S9. This was the same dispersion as in Fig. S1.

State	Viscosity (cP)	Intrinsic Viscosity	D_c (nm)	Std. Dev. in D_c (nm)	% Monomer by SEC
Pre-freezing	36±9	9	36	9	98.6
Post-freezing (1 month)	35	9	31	10	*
Post-freezing (2 ½ month	-	-	39	5	99.5

Sterile filtration of the clusters

A nanocluster dispersion were passed through a 0.22 micron filter membrane with ~220 mg/ml sheep IgG and 70 mg/ml trehalose as shown in Table S9 and Fig. S10. The dispersion properties including concentration of protein, viscosity and nanocluster size were retained after sterile filtration of the dispersion. The viscosity of the dispersion and the nanocluster size (36 nm) were low enough for sterile filtration to be feasible, which would be desirable for biopharmaceutical processing. Due to the large initial volume needed for filtration, the entire concentration process was carried out in a Millipore Amicon filter (used for buffer exchange as described in the materials and methods section).

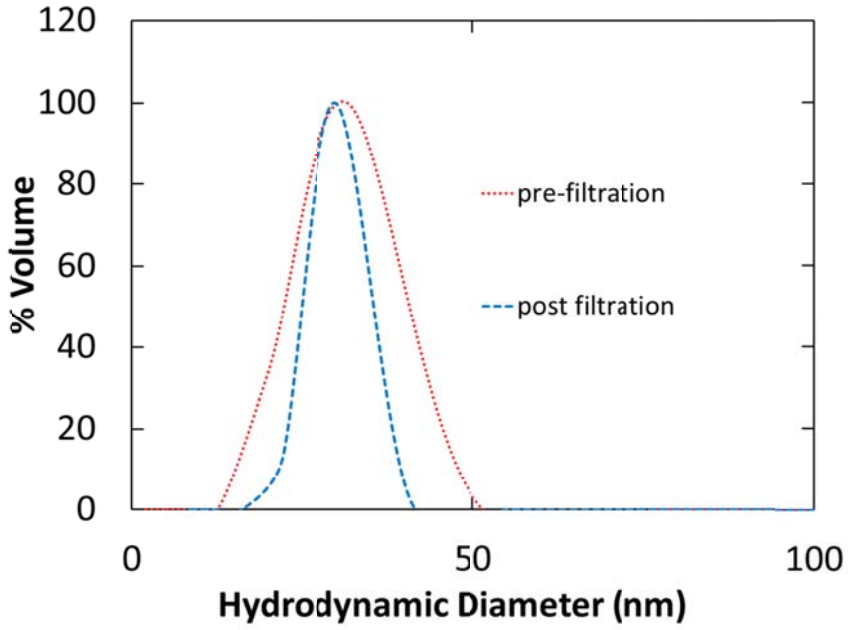

Figure S10: D_c of C 220:70 nanoclusters before and after sterile filtration through a 0.22 μm filter. The mean D_cs are listed in Table S9.

Table S9: D_c and viscosity of a C 220:70 nanocluster dispersion before and after sterile filtration through a 0.22 μm poyl(vinylidene difluoride) (PVDF) filter. The distributions for the D_cs are provided in Fig S10. The starting solution at a protein concentration of 48 mg/ml was centrifuged for 27 minutes. After forming the nanoclusters, a portion was saved and a portion was filtered. Both samples were then frozen, stored for a month and thawed, and then analyzed.

State of dispersion	*c* (mg/ml)	Viscosity (cP)	Intrinsic viscosity	D_c (nm)	St. Dev in D_c (nm)	% Monomer by SEC
Pre-filtration	220	36±9	9	33*	4.5	99.9
Post-filtration	200	26	10	30*	3.31	98.6

(1) Johnston, K. P.; Maynard, J. A.; Truskett, T. M.; Borwankar, A.; Miller, M. A.; Wilson, B.; Dinin, A. K.; Khan, T. A.; Kaczorowski, K. J. *Acs Nano* **2012**.
(2) Beenakker, C. W. J.; Mazur, P. *Physica A* **1984**, *126*, 349.
(3) Whitmore, L.; Wallace, B. A. *Biopolymers* **2008**, *89*, 392.
(4) Asakura, S.; Oosawa, F. *Journal of Polymer Science* **1958**, *33*, 183.

(5) Asakura S.; Oosawa F. *J. Chem. Phys.* **1954**, *22*.
(6) Tuinier, R.; Rieger, J.; De Kruif, C. G. *Advances in Colloid and Interface Science* **2003**, *103*, 1.
(7) Tessier, P. M.; Lenhoff, A. M. *Curr. Opin. Biotechnol.* **2003**, *14*, 512.
(8) Tessier, P. M.; Johnson, H. R.; Pazhianur, R.; Berger, B. W.; Prentice, J. L.; Bahnson, B. J.; Sandler, S. I.; Lenhoff, A. M. *Proteins-Structure Function and Genetics* **2003**, *50*, 303.
(9) Kulkarni, A. M.; Chatterjee, A. P.; Schweizer, K. S.; Zukoski, C. F. *J. Chem. Phys.* **2000**, *113*, 9863.
(10) Rosenbaum, D. F.; Zamora, P. C.; Zukoski, C. F. *Phys Rev Let* **1996**, *76*, 150.
(11) Lewus, R. A.; Darcy, P. A.; Lenhoff, A. M.; Sandler, S. I. *Biotechnol Prog* **2011**, *27*, 280.
(12) Chari, R.; Jerath, K.; Badkar, A. V.; Kalonia, D. S. *Pharmaceutical Research* **2009**, *26*, 2607.
(13) Harada, R.; Sugita, Y.; Feig, M. *J. Am. Chem. Soc.* **2012**, *134*, 4842.
(14) Groenewold, J.; Kegel, W. K. *J. Phys. Chem. B* **2001**, *105*, 11702.
(15) Groenewold, J.; Kegel, W. K. *J. Phys.-Condes. Matter* **2004**, *16*, S4877.
(16) Miller, D. P.; dePablo, J. J.; Corti, H. *Pharmaceutical Research* **1997**, *14*, 578.
(17) Moody, T. P.; Kingsbury, J. S.; Durant, J. A.; Wilson, T. J.; Chase, S. F.; Laue, T. M. *Analytical Biochemistry* **2005**, *336*, 243.
(18) Shire, S. J.; Shahrokh, Z.; Liu, J. *J. Pharm. Sci.* **2004**, *93*, 1390.
(19) Wang, B.; Tchessalov, S.; Warne, N. W.; Pikal, M. J. *Journal of Pharmaceutical Sciences* **2009**, *98*, 3131.